Functional universality and evolutionary diversity: insights from the structure of the ribosome

Ada Yonath[1,2*] and Francois Franceschi[3]

The structure of the mammalian ribosome, reconstructed at 25 Å resolution, has added a new dimension to our current knowledge, as it manifests the conservation and universality of the ribosome in respect to its primary tasks in protein biosynthesis. A combined approach to study of the ribosome, using X-ray crystallography and electron microscopy, may further improve our understanding of ribosome function in the future.

Addresses: [1]Max-Planck Unit for Structural Molecular Biology, 22603 Hamburg, Germany, [2]Department of Structural Biology, Weizmann Institute, Rehovot 76100, Israel and [3]Max-Planck Institute for Molecular Genetics, 14195 Berlin, Germany.

*Corresponding author.
E-mail: YONATH@MPGARS.DESY.DE

Structure 15 June 1998, **6**:679–684
http://biomednet.com/elecref/0969212600600679

Introduction

Ribosomes are universal cellular organelles facilitating the sequential polymerization of amino acids according to the blueprint encoded in the mRNA. Although they catalyze a rather simple chemical reaction, the formation of peptide bonds, the entire process of protein biosynthesis is highly complicated and depends on a large range of affinities, recognitions and selected interactions. In all organisms the ribosomes are giant ribonucleoprotein assemblies, constituted of two subunits of unequal size which associate upon the initiation of protein synthesis. Owing to their fundamental importance, the ribosomes have been the target of advanced biochemical and genetic research [1], as well as the subject of conventional electron microscopy studies, which have delineated the overall shape of the ribosome and highlighted several features on its surface [2,3].

During the past few years structural ribosomology has seen fascinating progress. This progress has resulted from almost two decades of work invested in the development of novel methodologies, based on single particle cryoelectron microscopy coupled with angular reconstitution and powerful computational procedures (such as multivariant statistics). These techniques have now come to fruition and have led to rather detailed visualization of the ribosomal structure. The popularity of reconstituted images stems from the ability to recognize in them the combination of the conventional surface topography alongside internal features, associated mainly with vacant spaces, such as tunnels and partially filled hollows. These were first detected about a decade ago in models obtained from negatively stained crystalline arrays of ribosomes [4,5].

Once the images of several smaller ribosomes, from prokaryotes [6,7] and yeast [8], had been reconstructed, the more complicated and larger particles from mammalian sources became the targets of similar studies, first at rather low resolution [9], and later at higher resolution. A recent study, focused on the rat liver ribosome at 25 Å resolution [10], revealed an incredible amount of structural information.

Conservation and universality

The remarkable similarity between the shape of a large part of the reconstructed images of the mammalian ribosome and those obtained from prokaryotes allowed the definition of a merged universal region [10]. The same high level of conservation is also manifested in the interior of the particles. For example, the void at the subunit interface, proposed to provide the site at which the main biosynthetic activity takes place [11–13], exists in eukaryotic as well as prokaryotic ribosomes [11–20]. Additional support for the conservation/universality view is given by the ability of tRNA molecules to interchange between all life kingdoms [13,19], despite their drastically different functional environments.

A prominent internal feature revealed in the mammalian 80S ribosome is a tunnel spanning the large subunit. The tunnel starts at a location assigned as the peptidyl transferase center and ends at a characteristic flat surface thought to be involved in docking the ribosome to the membrane of the endoplasmic reticulum (ER) [10]. This main tunnel can be correlated with that previously identified by reconstructions from crystalline arrays [5,13] of the prokaryotic large subunit (50S) and 80S ribosomes [4]; similar results were also seen in earlier studies performed using single-particle reconstructions [6,7,10,14–20]. It is striking that in the merged structure, obtained on the basis of matching the external characteristic features, the main large subunit tunnels were found to be structurally superimposed.

Although in early studies this tunnel was visualized at rather low resolution (28 Å), the characteristics and properties of this tunnel were consistent with it being the exit pathway for nascent protein chains, hence it was suggested to provide this function. Despite the logic of this assignment, at that time internal movement of the nascent protein was hard to conciliate, and this assignment stimulated much dispute of varying level: from the design of

Figure 1

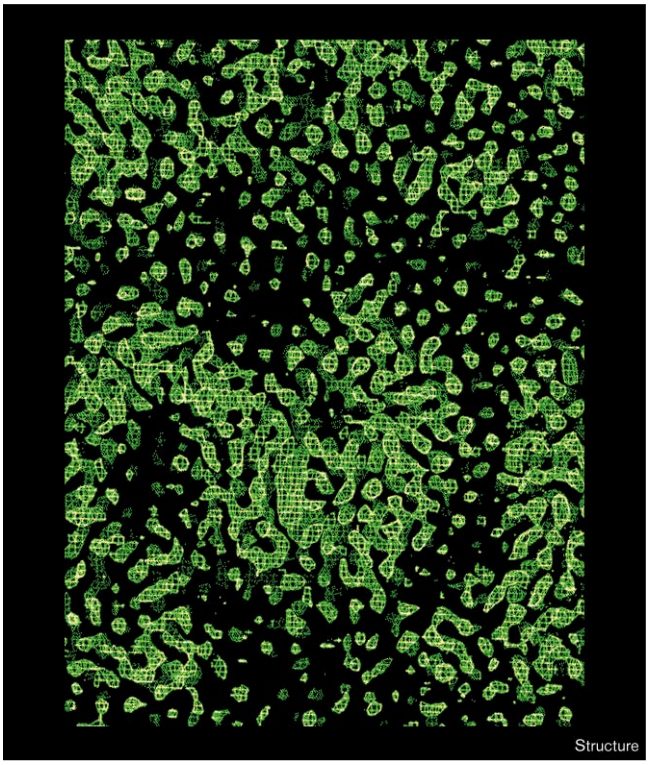

Part of the 12 Å electron-density map obtained for the large ribosomal subunit from *Haloarcula marismortui*, showing the entrance to the main internal tunnel (unit-cell dimensions = 211 Å × 300 Å × 567 Å; the crystals had $C222_1$ symmetry). This map was obtained by the multiple isomorphous replacement method, using crystals soaked in solutions containing 1–2 mM of $Ta_6Br_{14}Na_{16}$, $((O_3PCH_2PO_3)_4W_{12}O_{36})_nH_2O$, or $Cs_7(P_2W_{17}O_{61}Co(NC_5H_5))_nH_2O$).

semi-supportive experiments [21] via counter propositions [22] to ignorance of the concept of conservation of the main ribosomal functions. Thus, assuming (mistakenly) that the tunnel was detected in a halophilic ribosome, its existence was suggested to stem from the extreme conditions under which these bacteria grow [23]. It was almost a decade before the tunnel concept became widely accepted, primarily owing to its detection in the higher resolution images reconstructed from single particles [6,7,10,14–20]. Recently the universality of this tunnel has been extended to archae, as it was detected in a 12 Å electron-density map obtained by model-free X-ray crystallography studies on crystals of the large ribosomal subunit from *Haloarcula marismortui* (Figure 1) [24].

Single-particle reconstruction studies recently provided direct evidence that this tunnel is indeed the exit path of nascent proteins [17]. These studies showed density corresponding to a quasi-pentagonal circular structure of Sec61 [25], the pore providing the path for the nascent chain during translocation through the ER membrane, connected to a funnel located at the end of the tunnel of yeast ribosomes. This funnel matches a similar feature detected earlier in prokaryotic large ribosomal subunits. As it was observed that several proteins may undergo co-translational folding, and as there is no obvious counterpart for the ER membrane in prokaryotic cells, this funnel was suggested to provide the site at which partial or complete folding may take place (Figure 2) [26].

Evolution and diversity

Apart from some peripherally located additional features on the surfaces of the two subunits, presumably involved in specific recognition events, the most noticeable difference between the mammalian 80S and the prokaryotic 70S ribosomes is in a substantial increase in mass on one side of the 60S subunit. Together with the conserved core of the ribosome, this extra portion creates a most striking large flat region, named the 'flat ribosomal surface' (FRS) [10]. As the tunnel, described above, was found to be almost perpendicular to the FRS, the FRS is assigned to be the structural element required for docking at the ER membrane. Thus, from the structural point of view it seems that the extra mass of the 80S ribosomes is designed to provide the ribosome with a stable membrane interface area, that is important for translocation of the nascent chains as well as for ribosome preservation. Thus, the topology of the FRS may facilitate the efficient *in vivo* formation of periodic organizations of ribosomes in eukaryotic cells under stressful conditions [13]. This organization is believed to be the physiological mechanism for temporary storage of ribosomes, aimed at preserving their integrity and activity in preparation for the expected better conditions in the future.

The comparison of the FRS with the non-even shape of the prokaryotic ribosomes may provide an explanation for the extreme difficulties encountered in attempts to produce well ordered large arrays of the latter [27]. In fact, even the readily grown salt-stabilized crystalline sheets of prokaryotic ribosomes [5,11] were found to be insufficiently stable to undergo cryogenic treatment, which could have led to reconstructions at similar, or even higher, resolution than those currently obtained by single-particles reconstructions.

Structures without crystals?

The recent increase in the number and quality of single-particle reconstructions shows that imaging ribosomal particles at 15–25 Å has become almost routine. The elegant exploitation of these reconstructions in comparative studies between empty ribosomes and their complexes, mimicking active or 'stalled' stages in the biosynthetic process has opened new horizons [14–20]. In favorable cases, the structures of the non-ribosomal components in the functional complexes have been determined crystallographically (e.g. the structure of tRNA and a ternary

complex of the elongation factor [14–16,19,20]) or by image reconstruction (e.g. Sec61 [25]). Therefore, the lower resolution shapes of these components can be well approximated and spotted in the difference maps rather easily. However, although the resolution limits of these studies are sufficient to reveal locations and gross orientational parameters, they are insufficiently detailed to establish unambiguously the fine details of interactions or movements. Hence, it is no wonder that there are frequent discrepancies in the interpretations provided by different laboratories. Experience in the ribosome field, however, shows that such discrepancies are usually reconsidered and refitted in later stages.

Are we witnessing the foundations of crystallography without crystals? At a first glance it seems to be so, as structures are emerging independent of the availability of crystalline samples. Although the leaders of this field expect further progress, it is not clear that electron microscopy of large particles will reach the crystallographic level of detail, however. Furthermore, even at comparable resolution, there are major conceptual differences between reconstructed and crystallographically determined structures, some of which are discussed below.

Among the factors most influential in the growth of well diffracting crystals is the requirement for conformational homogeneity. Obviously, this requirement hampers the crystallization of many flexible and unstable macromolecular assemblies. The reconstruction methods provide relief from this stringent requirement but at the same time, even when the level of conformational heterogeneity is so low that it is hardly noticed by the mathematical treatment (e.g. for conformational variations of the same order of magnitude as the resolution limits), the averaging of the images of mixed populations reduces the quality of the resulting images. The requirement for quantitative homogeneity is especially important for the investigation of functional complexes, as each ribosomal preparation usually contains a large portion of inactive particles. Dividing samples into subgroups may provide some help [19], but it should not be forgotten that this is a rather subjective criterion.

A weak aspect of the single-particle methods is the choice of threshold levels; these are chosen primarily at two stages in the course of the reconstruction. The first has to do with the term 'resolution' which has a different meaning to that used in X-ray crystallography. In the latter method

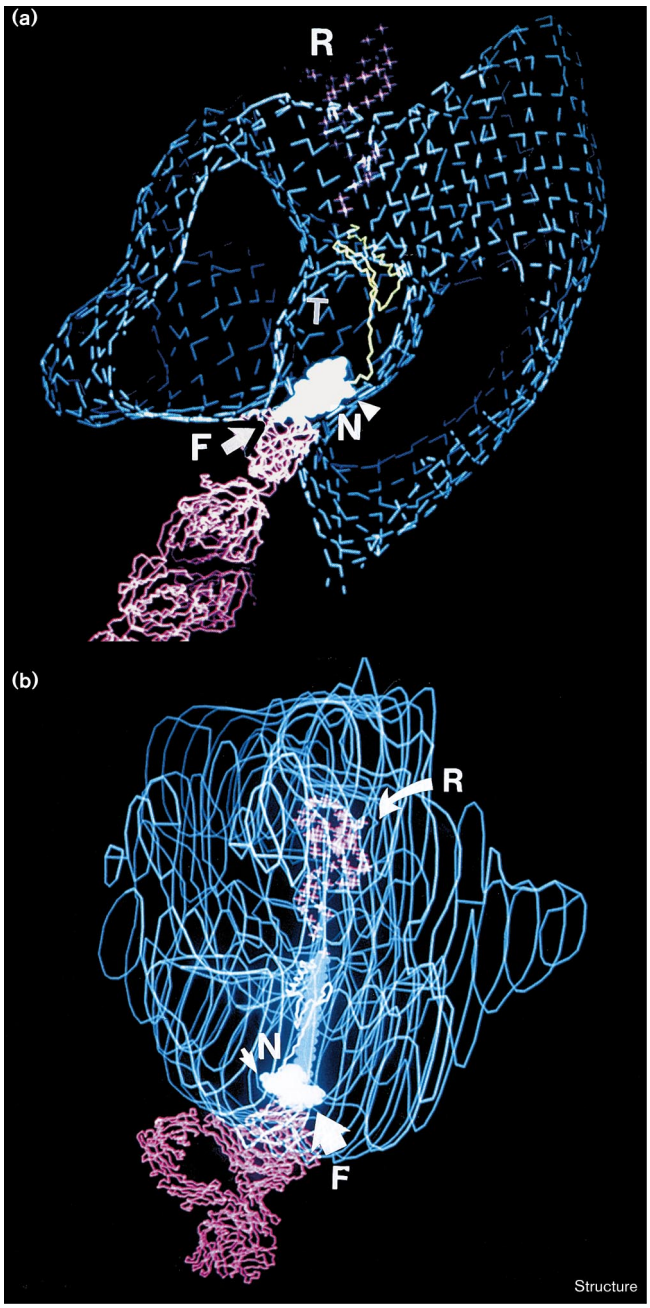

Figure 2

A feasible path for the partial folding of small proteins synthesized *in vitro*. **(a)** A slice within the 50S ribosomal subunit (in blue), into which the crystallographically determined structure of the mainchain of the MS2 viral coat protein [34] was model-built. The protein (drawn as a Cα trace) was placed along the tunnel maintaining the native fold of its β sheet domains and the segment (residues 1–47) of its N terminus (called N, drawn together with the sidechains as a space-filling model). The protein was positioned so as to allow free movement at the hinges between the structural domains. The C terminus of MS2 was placed in the vicinity of the suggested peptidyl transferase center and the N terminus (N) in the funnel (F) located in the exit domain of the tunnel (T). A tRNA molecule (R) was placed in a void at the subunit interface so that its anticodon loop is in the proximity of the groove proposed as the mRNA-binding site and its CCA end points into the entrance to the tunnel. A hypothetical IgG molecule (in pink) was attached to the N terminus of the protein at the funnel (end of the tunnel), so as to make the closest possible contacts with the ribosome (for rational see [33]). **(b)** The envelope of the whole 70S ribosome is shown as a blue 'transparent' line, with assignments as in (a).

Figure 3

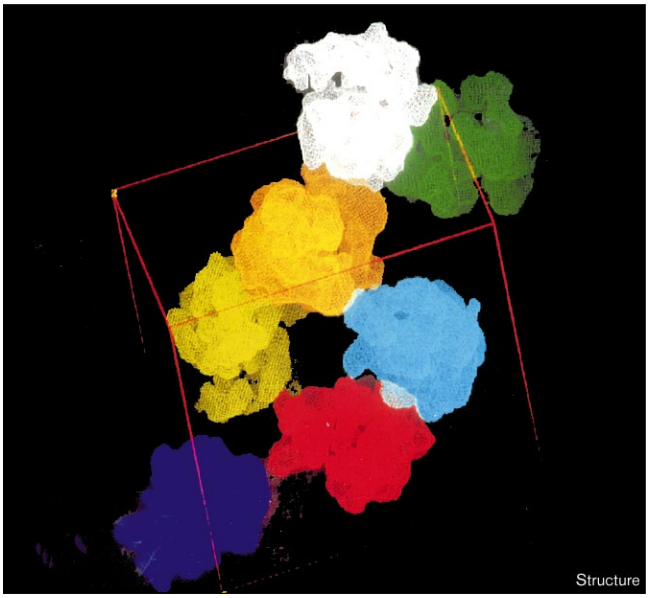

The packing diagram of the crystallographic unit cell of the 70S ribosome from *T. thermophilus*. The 23 Å electron microscopical model of this particle (H Stark and M van Heel, unpublished results) was positioned in the crystallographic unit cell according to the most prominent result of the molecular replacement search, and eight symmetry operations were applied. Each particle is shown in a different color. Crystallographic data were collected at beamline BW6/DESY to 17 Å resolution.

this is a solid value, determined simply by the extent of the diffraction patterns and reflecting the extent of the crystal's internal order. In the reconstruction methods, however, resolution relates to the (still not agreed upon) cut-off value of the Fourier-shell correlation as a function of the spatial frequency, or a combination of it and the signal-to-noise ratio [10,19].

The second parameter sensitive to the threshold definition relates to the choice of the contouring level of the reconstructed image. In X-ray crystallography the outer border is determined by the locations of the individual atoms and the contour is precisely defined by the number of electrons per unit volume. In reconstructions from crystalline sheets, the size of the resulting image is determined by the distribution of the density coupled with the unit-cell dimensions, which set the upper and lower limits. The threshold definition in single particle image reconstruction depends on the chosen computational procedures as well as a combination of biochemical and functional considerations. Such an approach is prone to lead to less accurate figures, which in turn may show significant discrepancies in the volume of the resulting images. The sensitivity of the volume to small variations is noteworthy as small linear inaccuracies may lead to substantial differences in volume estimation (e.g. a 10% linear reduction leads to an image of about 70% of the initial volume). It is therefore clear why the initial reconstructed images [6,7] of the ribosome were of rather different sizes, although their overall shapes and their prominent external and internal features seemed to be similar. Nevertheless, with the advances in computational methods and the inclusion of a larger number of particles into the statistical set, these discrepancies have been settled and currently all the reconstructed prokaryotic ribosomes, including those obtained from two-dimensional sheets of single particles, are of similar volumes: 3.16×10^6 Å^3, 2.9×10^6 Å^3 and 3.4×10^6 Å^3, for 70S ribosomes reconstructed form crystalline arrays [11] and single particles [6,7], respectively.

The inherent uncertainties in choosing the right threshold levels may also lead to differences in the shape of a structure. This was well illustrated in the structure determination of the *Escherichia coli* large ribosomal subunit using random-conical reconstructed images [2,3,28]. The threshold was chosen so that the extended conformation of the flexible L7/L12 arm (where L7 and L12 are two ribosomal proteins) was maintained, as at that time this was the fashionable view. At this threshold, the structure revealed two internal holes with no apparent function. Interestingly, if a slightly higher threshold had been used, these two holes may have been seen to be connected to form an internal tunnel, comparable to the structurally conserved feature described above [28]. At the lower contour level, however, the L7/12 arm appeared in a conformation similar to that observed in all reconstructions of crystalline arrays [5,13] as well as in all reconstructions from ice-embedded single particles [6,7,10,14–20].

The interplay between microscopy and crystallography

The dream of 'crystallography' with no crystals may never be true. In studies of large macromolecular assemblies, however, the interplay between image reconstruction and X-ray crystallography should be extremely fruitful. In the field of ribosome research merged electron microscopy and X-ray studies may assist the crucial step of phasing, as serious obstacles have been encountered in attempts to phase data collected from ribosomal crystals diffracting to rather high resolution [24]: 2.7 Å (from the *H. marismortui* 50S subunit) and 3.4 Å (from the *T. thermophilus* 30S subunit). Thus, the packing arrangement of the crystals of the 70S ribosome (Figure 3) and the 50S ribosomal subunit (Figure 4) from *Thermus thermophilus* have been elucidated [24] (H Stark and M van Heel, unpublished results) using reconstructed images of these particles. Despite the current success of this 'hybrid' approach, it remains to be seen to what extent an envelope with a Gaussian distribution of intensities and rather limited resolution can reproduce crystallographic amplitudes.

An additional aspect for constructive interactions between the two methods of structure determination can be

Figure 4

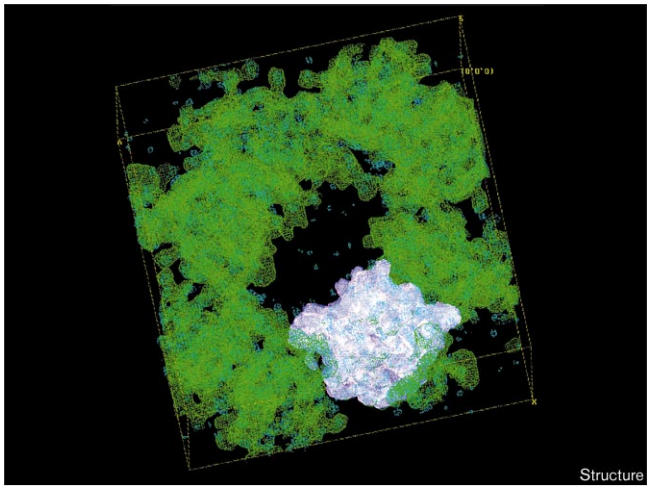

The content of the crystallographic unit cell of the large ribosomal subunit (50S) from *T. thermophilus*, assembled by positioning the reconstructed model in the crystallographic unit cell according to the most prominent result of the molecular replacement search and the symmetry of the crystal. Structure-factor amplitudes were measured at beamline BW6/DESY to 9 Å resolution. Phases were calculated by back transformation of the assembled map. One asymmetric unit, which corresponds to one ribosomal particle, is marked in pink. The map calculated from the assembled particles is shown in green, and that constructed from the crystallographic amplitudes and the model phases is in cyan. The green patches (on top of the pink model) and the cyan patches which coincide with them, are parts of the neighboring particles. The 'only cyan' patches indicate differences in the structure between the observed and calculated particles.

envisaged. The current structural knowledge of the ribosome, inferred principally from images of entire particles derived from electron microscopy, can be combined together with the structures of isolated 'bits and pieces' of the ribosome (e.g. individual ribosomal proteins, rRNA etc.) determined by crystallographic and/or NMR investigations. It is not surprising that the relatively high level of detail observed recently tempted the fitting of ribosomal components of known structure, such as ribosomal protein L1 [19], or those that can be approximated to known structures, such as double-stranded rRNA [6,19,29]. Experience has shown that when such attempts are based solely on visualization, with no supporting structural information (e.g. differences in densities), they are rather premature and may easily lead to over-interpretation [24].

Of interest is an exercise that attempted to fit the coordinates of a ribosomal protein, L1 from *T. thermophilus* [30], into the electron-density map of the *T. thermophilus* 50S subunit, constructed at 16 Å from the crystallographically measured structure factors and phases obtained by molecular replacement of the image of exactly the same particles. This exercise led to two alarming findings. The first is connected to a number of reasonable fits obtained when the coordinates of the protein were manually placed in several orientations within the region assigned to be in the proximity of protein L1 by imunoelectron-microscopy. The second relates to a rather primitive molecular search performed throughout the ribosomal particle, which revealed additional positions into which the same structure could be fitted equally well, indicating clearly that unambiguous positioning of ribosomal components is still not recommended. This study also confirmed that protein L1 contains a popular RNA-binding motif, found so far in several ribosomal proteins [31].

Additional uncertainties associated with such placements relate to the open questions concerning the validity of using the conformations of ribosomal components determined in isolation to represent the *in situ* situation. Within the ribosome it is possible that the conformations of individual components may be highly influenced by their proximities to other ribosomal proteins or rRNA. The case of protein S15 [32], which shows significant conformational variability should not be ignored. Nevertheless, although still not ripe for detailed investigations, extrapolating from the advances made so far and from their potential coupling with crystallographic results, there are legitimate solid expectations that the molecular structure of the ribosome will be determined in the foreseeable future. Meanwhile, it is certain that the impressive series of reconstructions will keep increasing and further assignments, refinements and rearrangements are just behind the door. Thus it is clear that much intriguing work still lies ahead.

Acknowledgements

The images of the thermophilic ribosome and its large subunit were reconstructed by H Stark and M van Heel. The EM diffraction studies were performed at the Weizmann Institute, Rehovot, the Max-Planck Research Unit in Hamburg, the Max-Planck Institute for Molecular Genetics in Berlin and EMBL, Heidelberg. We thank Kevin Leonard and all members of these research groups for their collaboration and advice. Support was provided by the US National Institute of Health (NIH GM 34360), the German Ministry for Science and Technology (BMBF 05-641EA) and the Kimmelman Center for Macromolecular Assembly at the Weizmann Institute. AY holds the Martin S Kimmel Professorial Chair.

References

1. Green, R. & Noller, H. (1997). Ribosomes and translation. *Annu. Rev Biochem.* **66**, 697-716.
2. Radamacher, M., Wagenknecht, T., Verschoor, A. & Frank, J. (1987). Three-dimensional structure of the large ribosomal subunit from *E. coli*. *EMBO J.* **6**, 1107-1114.
3. Frank, J., Verschoor, T., Radamacher, M. & Wagenknecht, T. (1990). Morphologies of eubacterial and eukaryotic ribosomes detected by three-dimensional electron microscopy. In *Ribosome, Structure, Function and Evolution.* (Hill, W.E., *et al.*, Warner, T.A. eds.), pp. 107-113, ASM Press, Washington DC.
4. Milligan, R. & Unwin, P.N.T. (1986). Location of the exit channel for nascent proteins in 80S ribosomes. *Nature* **319**, 693-696.
5. Yonath, A., Leonard, K.R. & Wittmann, H.G. (1987). A tunnel in the large ribosomal subunit revealed by three-dimensional image reconstruction. *Science* **236**, 813-816.
6. Stark, H., *et al.*, & Van Heel, M. (1995). The 70S *E. coli* ribosome at 23 Å resolution: fitting the ribosomal RNA. *Structure* **3**, 815-821.
7. Frank, F., *et al.*, & Agrawal, R.K. (1995). A model of protein synthesis based on cryo electron microscopy of the *E. coli* ribosome. *Nature* **376**, 441-444.

8. Verschoor, A., Warner, J.R., Srivastava, S., Grassucci, R.A. & Frank, J. (1998). Three-dimensional structure of the yeast ribosome. *Nucleic Acids Res.* **26**, 655-661.
9. Verschoor, A., Srivastava, S., Grassucci, R. & Frank, J. (1996). Native 3D structure of eukaryotic 80s ribosome: morphological homology with the *E. coli* 70S ribosome. *J. Cell Biol.* **133**, 495-505.
10. Dude, P., *et al.*, & van Heel, M. (1998). The 80S rat liver ribosome at 25 Å resolution by electron microscopy and angular reconstruction. *Structure* **6**, 398-399.
11. Arad, T., Piefke, J., Weinstein, S., Gewitz, H.S., Yonath, A. & Wittmann, H.G. (1987). Three-dimensional image reconstruction from ordered arrays of 70S ribosomes. *Biochimie* **69**, 1001-1006.
12. Hansen, H.A.S., *et al.*, & Yonath, A. (1990). Crystals of complexes mimicking protein biosynthesis are suitable for crystallographic studies. *Biochem. Biophys. Acta* **1050**, 1-5.
13. Berkovitch-Yellin, Z., Bennett, W.S. & Yonath, A. (1992). Aspects in structural studies on ribosomes. *CRC. Rev. Biochem. Mol. Biol.* **27**, 403-444.
14. Agrawal, K.R., *et al.*, & Frank, J. (1996). Direct visualization of A-, P-, and E-site tRNA in the *E. coli* ribosome. *Science* **271**, 1000-1002.
15. Stark, H., *et al.*, & van Heel, M. (1997). Arrangement of the tRNAs in pre- and posttranslational ribosomes revealed by electron cryomicroscopy. *Cell* **88**, 19-28.
16. Stark, H., Rodina, M.V., Rinke-Appel, J., Brimacombe, R., Wintermeyer, W. & van Heel, M. (1997). Visualization of elongation factor Tu in the *E. coli* ribosomes. *Nature* **389**, 403-406.
17. Beckmann, R., *et al.*, & Frank, J. (1997). Alignment of conduits for the nascent polypeptide chain in the ribosome–Sec61 complex. *Science* **278**, 2123-2126.
18. Verschoor, A., Warmer, J.R., Srivastava, S., Grassucci, R. & Frank, J. (1997). 3D structure of the yeast ribosome. *Nucleic Acids Res.* **26**, 655-661.
19. Malhotra, A., *et al.*, & Frank, J. (1998). *E. coli* 70S ribosome at 15 Å resolution by cryo-electron microscopy: localization of fMet–tRNA$_f^{Met}$ and fitting of L1 protein. *J. Mol. Biol.*, in press.
20. Agrawal, K.R., Penczek, P., Grassucci, R.A. & Frank, J. (1998). Visualization of the elongation factor G on *E. coli* 70S ribosome: the mechanism of translation. *Proc. Natl Acad. Sci. USA*, in press.
21. Kurzchalia, S.V., Wiedmann, M., Breter, H., Zimmermann, W., Bauschke, E. & Rapoport, T.A. (1988). tRNA-mediated labeling of proteins with biotin, a nonradioactive method for the detection of cell-free translation products. *Eur. J. Biochem.* **172**, 663-668.
22. Ryabova, L.A., Selivanova, O.M., Baranov, V.I., Vasiliev, V.D. & Spirin, A.S. (1988). Does the channel for nascent peptide exist inside the ribosome? *FEBS Lett.* **226**, 255-260.
23. Moore, P. (1988). The ribosome returns. *Nature* **331**, 223-227.
24. Harms, J., *et al.*, & Yonath, A. (1998). The quest for the molecular structure of a large macromolecular assembly exhibiting severe non-isomorphism, extreme beam sensitivity and no internal symmetry. *Acta Cryst.*, in press.
25. Hanein, D., *et al.*, & Akey, C.W. (1996). Oligomeric ring of the Sec61 complex induced by ligand required for protein translocation. *Cell* **87**, 721-732.
26. Eisenstein, M., *et al.*, & Yonath, A. (1994). Modelling the experimental progression of nascent protein in ribosomes. In *Supramolecular Structure and Function.* (Pifat, G., ed.), Vol. 4, pp. 213-244, Balaban Press, Rehovot, Israel.
27. Avila-Sakar, A.J., *et al.*, & Chiu, W. (1994). Electron cryomicroscopy of *B. stearothermophilus* 50S ribosomal subunits crystallized on phospholipid monolayer. *J. Mol. Biol.* **239**, 689-697.
28. Yonath, A. & Berkovitch-Yellin, Z. (1993). Hollows, voids, gaps and tunnels in the ribosome. *Curr. Opin. Struct. Biol.* **3**, 175-180.
29. Mueller, F. & Brimacombe, R. (1997). A new model for the three-dimensional folding of *E. coli* 16S RNA. I. Fitting of the RNA to 3D electron microscopical map at 20 Å resolution. *J. Mol. Biol.* **271**, 524-544.
30. Nikonov, S., *et al.*, & Liljas, A. (1996). Crystal structure of the RNA binding ribosomal protein L1 from *Thermus thermophilus*. *EMBO J.*, **15**, 1350-1359.
31. Liljas, A. & Al-Karadaghi, S. (1997). Structural aspects of protein synthesis. *Nat. Struct. Biol.* **4**, 767-771.
32. Clemons, W.M., Davies, C., White, S. & Ramakrishnan, V. (1998). Conformational variability of the N-terminal helix in the structure of ribosomal protein S15. *Structure* **6**, 429-438.
33. Valegard, K., Liljas, L., Friborg, K. & Unge, T. (1990). The three-dimensional structure of the bacterial virus MS2. *Nature* **345**, 36-41.